Sensitivity Analysis Using Adjoint Parabolized Stability Equations for Compressible Flows

J.O. Pralits (jpralits@mech.kth.se)
Department of Mechanics, KTH, SE-100 44 Stockholm, Sweden

C. Airiau (christophe.airiau@imft.fr)
Institut de Mécanique des Fluides de Toulouse, Allée du professeur Camille Soula, F-31 400 Toulouse, France

A. Hanifi (hia@ffa.se) and D.S. Henningson (hnd@ffa.se)*
Swedish Defence Research Agency, FOI, Aeronautics Division, FFA, SE-172 90 Stockholm, Sweden

Abstract. An input/output framework is used to analyze the sensitivity of two- and three dimensional disturbances in a compressible boundary layer for changes in wall- and momentum forcing. The sensitivity is defined as the gradient of the kinetic disturbance energy at a given downstream position with respect to the forcing. The gradients are derived using the parabolized stability equations (PSE) and their adjoint (APSE). The adjoint equations are derived in a consistent way for a quasi two-dimensional compressible flow in an orthogonal curvilinear coordinate system. The input/output framework provides a basis for optimal control studies. Analysis of two-dimensional boundary layers for Mach numbers between 0 and 1.2 show that wall- and momentum forcing close to branch I of the neutral stability curve give the maximum magnitude of the gradient. Forcing at the wall gives the largest magnitude using the wall normal velocity component. In case of incompressible flow, the two-dimensional disturbances are the most sensitive ones to wall inhomogeneity. For compressible flow, the three-dimensional disturbances are the most sensitive ones. Further, it is shown that momentum forcing is most effectively done in the vicinity of the critical layer.

Keywords: adjoint, PSE, sensitivity, boundary layer stability, compressible

1. Introduction

Transition from laminar to turbulent flow can be triggered by unstable disturbances inside the boundary layer. The growth of such disturbances are known to be sensitive to surface inhomogeneities, forcing inside the boundary layer and external acoustic perturbations, see *e.g.* Nishioka and Morkovin (1986), Saric (1993) and Corke, Bar-Sever and Morkovin (1986). The studies devoted to the birth of disturbances due to such forcing are called receptivity. The acoustic receptivity is explained by Goldstein (1983) as a wavelength conversion mechanism.

* also at Department of Mechanics, KTH, SE-100 44 Stockholm, Sweden

The long wave length of an acoustic wave can be converted to a shorter wave length of an instability wave at the leading edge or where a geometric inhomogeneity is present. Results of boundary layer receptivity are documented by Crouch (1992a, 1992b) and Choudhari and Street (1992) for two-dimensional disturbances in a Blasius boundary layer. Other references may be found in Goldstein (1989) and in Saric (1993).

A disturbance inside the boundary layer may encounter an unsteady wall inhomogeneity (forcing) which changes its growth. This problem can also be viewed as a receptivity to wall perturbations. If the perturbation is appropriate, it can be used to control the development of the disturbance. This is the wave cancellation concept proposed by Thomas (1983). Such study may be formulated as input/output problem where the input is some forcing on the wall or in the boundary layer, and the output is a measure of the disturbance in the domain. The sensitivity can be defined as the gradient of the output with respect to the input. A typical output measure is the disturbance energy at some downstream position or in the whole domain. Such a formulation can easily be extended to a control problem by using the gradient to update the input *i.e.* control variables in order to minimize the output. This analysis can be done with gradient based optimization techniques as shown in Gunzburger (2000) and Bewley, Temam and Ziane (2000).

Here we investigate the sensitivity of disturbances to unsteady wall conditions and source of momentum in a compressible boundary layer in framework of the non-local stability theory. This analysis is formulated as an input/output problem and provides information which is useful for the control of disturbances. The state equations are the so called Parabolized Stability Equations, PSE, and are written in an orthogonal curvilinear coordinates system. For a detailed presentation of PSE see *e.g.* Bertolotti, Herbert and Spalart (1992) and Simen (1992).

The main tool developed here is based on the adjoint equations. The approach of adjoint equations has been used for sensitivity studies in oceanography and atmospheric circulation models, *e.g.* Hall (1986). This approach has also appeared in receptivity studies. Tumin (1996) used it for confined flows. Hill (1995, 1997) applied the adjoint approach for the local and nonlocal stability theories to study the receptivity of Tollmien-Schlichting waves in boundary layer flows. Receptivity of Görtler vortices was studied by Luchini and Bottaro (1998) using backward-in-time integration. The adjoint techniques has also been used for identifying the optimal disturbances in boundary layer flows, *e.g.* Andersson, Berggren and Henningson (1999) and Luchini (2000).

Sensitivity analysis may be performed by forward calculations. For each parameter that is changed (inhomogeneous wall boundary conditions, initial disturbance, momentum source) the forward problem has

to be solved. The total time spent will be the product of the number of input parameters and the time spent for each calculation.

The advantage of the adjoint approach is that the sensitivity of a disturbance can be obtained by solving the state and adjoint equations once. This means that the adjoint method can provide an optimal distribution of suction to suppress the growth of disturbances with a relatively low computational cost. Such a study was carried out by Cathalifaud and Luchini (2000) for optimal disturbances in a Blasius boundary layer.

The aim of the present work is to derive the adjoint of the parabolized stability equations for a compressible flow in a consistent way. The paper is organized as follows. In section 2 the problem is defined and section 3 gives the adjoint formulation and the gradient expressions. Validation and results of the sensitivity analysis are presented for a two-dimensional compressible boundary layer with two and three dimensional disturbances in section 4. The conclusions appear in section 5. Details of the derivation of nonlocal stability equations and their adjoint are given in the appendix.

2. Problem formulation

2.1. Definition of the sensitivity

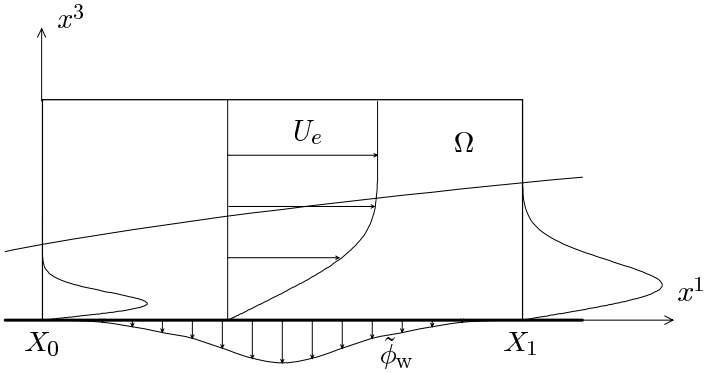

Figure 1. Computational domain

The sensitivity of two- and three dimensional disturbances in a compressible boundary layer for changes in wall- and momentum forcing is investigated. This analysis is formulated as an input/output problem and will be discussed below considering the domain given in figure 1. Here, x^1, x^2 and x^3 are the streamwise, spanwise and wall normal coordinates, respectively, and U_e the freestream velocity. The computational domain is defined such that $x^1 \in [X_0, X_1]$, $x^2 \in [Z_0, Z_1]$ and

$x^3 \in [0, \infty[$. An initial disturbance is superimposed to the boundary layer base flow at an upstream position X_0.

In optimal control theory, sensitivity is defined as the derivative of the state variables (output) with respect to the control variables (input). It is related to the gradient of a functional J (called cost or objective functional) which includes both a measure of a state E and a measure of the control E_c. The measures are weighted together with a positive factor ϵ, so called the regularization parameter, as $J = E + \epsilon E_c$. The regularization parameter serves the purpose of limiting the size of the control. The optimal input can then be obtained via an optimality condition using gradient based optimization techniques as *e.g.* steepest descent or conjugate gradient, see *e.g.* Bewley *et al.* (2000) and Gunzburger (2000).

Here, the input is defined as the inhomogeneities of velocity $\tilde{\mathbf{u}}_\mathrm{w}$ and temperature $\tilde{T}_\mathrm{w}$ on the wall $x^3 = 0$ and a source $\tilde{\mathcal{S}}$ in the boundary layer. The output is a function of disturbance variables, here written as the disturbance energy norm

$$E = \frac{1}{2} \int_{Z_0}^{Z_1} \int_0^\infty \tilde{\phi}_1^H \mathcal{M} \tilde{\phi}_1 h_2 h_3 \, dx^3 \, dx^2, \tag{1}$$

or alternatively

$$E = \frac{1}{2} \int_{X_0}^{X_1} \int_{Z_0}^{Z_1} \int_0^{+\infty} \tilde{\phi}^H \mathcal{M} \tilde{\phi} \, h_1 h_2 h_3 \, dx^1 \, dx^2 \, dx^3, \tag{2}$$

where $\tilde{\phi} = (\tilde{\rho}, \tilde{u}, \tilde{v}, \tilde{w}, \tilde{T})^\mathrm{T}$ with $\tilde{\rho}$ denoting the density perturbation, $\tilde{u}, \tilde{v}, \tilde{w}$ the streamwise, spanwise and normal velocity perturbations, respectively, and $\tilde{T}$ the temperature perturbation. The superscript ^{H} denotes the transpose complex conjugate, the subscript $_1$ refers to values at $x = X_1$ and h_i the scale factors of the coordinate system. The positive diagonal matrix $\mathcal{M}$ defines the measure of 'size' of disturbances. In this paper $\mathcal{M} = \mathrm{Diag}(0, 1, 1, 1, 0)$ such that disturbances are measured by the modulus of their velocity components. An example of another measure is given in Hanifi *et al.* (1994) where $\mathcal{M} = \mathrm{Diag}(T/\rho\gamma M^2, \rho, \rho, \rho, \rho/\gamma(\gamma-1)TM^2)$ with T being the mean temperature, ρ the mean density, γ the ratio of the specific heat coefficients and M the Mach number of the flow. We define the sensitivity as the gradient of E with respect to $\tilde{\mathbf{u}}_\mathrm{w}$, $\tilde{T}_\mathrm{w}$ and $\tilde{\mathcal{S}}$. Here we consider the case with no penalty, *i.e* $\epsilon = 0$, therefore can the output be written $J = E$.

In the present paper the amplitude of the control parameters are assumed to be so small that the nonlinear interaction with the mean flow can be neglected. However, the procedure presented here can be

extended to account for the modification of the mean flow, see Pralits *et al.* (2000).

2.2. State equations

The governing equations are the non-local stability equations formulated using PSE technique for quasi-three dimensional viscous, compressible flow formulated in primitive variables and general, orthogonal curvilinear coordinates. Here, we consider a general case where the boundary layer is subjected to sources of mass, momenta and energy $\tilde{\mathcal{S}}$, and inhomogeneous boundary conditions on the wall $\tilde{\mathbf{u}}_{\mathrm{w}}$ and $\tilde{T}_{\mathrm{w}}$. The notation, the reference quantities, the assumptions and the derivation of the PSE are given in appendix A. The equations in symbolic form are written as

$$\begin{aligned}
\hat{\mathcal{L}}\,\hat{\phi} &= \hat{\mathcal{S}} && \text{in } \Omega \\
\hat{\phi} &= \hat{\phi}_0 && \text{on } x^1 = X_0 \\
\hat{\mathbf{u}} = \hat{\mathbf{u}}_{\mathrm{w}}(x^1), \quad \hat{T} &= \hat{T}_{\mathrm{w}}(x^1) && \text{on } x^3 = 0 \\
\hat{\mathbf{u}} \to 0, \quad \hat{T} &\to 0 && \text{as } x^3 \to \infty \\
\int_0^\infty \hat{\phi}^H \frac{\partial \hat{\phi}}{\partial x^1}\, h_2 h_3 dx^3 &= 0 && \forall\ x^1
\end{aligned} \tag{3}$$

The disturbance $\tilde{\phi}$, the source $\tilde{\mathcal{S}}$ and the inhomogeneous boundary conditions have been divided into an amplitude function and a wave function

$$\tilde{\phi}(x^i,t) = \hat{\phi}(x^1,x^3)\Theta, \quad \tilde{\mathcal{S}}(x^i,t) = \hat{\mathcal{S}}(x^1,x^3)\Theta, \tag{4}$$

where

$$\Theta(x^1,x^2) = \exp\, i\,(\int_{X_0}^{x^1} \alpha(x')dx' + \beta x^2 - \omega t). \tag{5}$$

Here, α is the complex streamwise wavenumber, β the real spanwise wavenumber and ω the real angular frequency of the perturbations. The integral expression in equation (3), the so called auxiliary condition, is used to remove the ambiguity from the streamwise dependence that remains between the wave and the amplitude functions.

In accordance to the derivation of the nonlocal stability equations, the input parameters ($\hat{\mathbf{u}}_{\mathrm{w}}$, $\hat{T}_{\mathrm{w}}$ and $\hat{\mathcal{S}}$) are assumed to be weak functions of the streamwise coordinate, *i.e.* $\partial/\partial x^1 \sim \mathcal{O}(R^{-1})$. Note that $\tilde{\phi}_{\mathrm{w}}$ and $\tilde{S}$ have the same x^2, t and main x^1 dependence as the disturbances.

The system of equations (3), which is nonlinear in $(\alpha, \hat{\phi})$, is integrated in the downstream direction using a marching procedure, with the initial condition at $x^1 = X_0$ given by the local stability theory. At

each streamwise position, the value of α is iterated such the auxiliary condition is satisfied.

3. Adjoint equations and gradients

The gradient of the output given by (1), is defined through the directional derivative as

$$\begin{aligned}\delta J = \quad & \texttt{Real}\left\{\int_{X_0}^{X_1}\int_{Z_0}^{Z_1}\left(\nabla_{\tilde{\mathbf{u}}_\mathrm{W}} J^H \delta\tilde{\mathbf{u}}_\mathrm{W} + \nabla_{\tilde{T}_\mathrm{W}} J^H \delta\tilde{T}_\mathrm{W}\right) h_1 h_2 \, dx^2 \, dx^1 + \right. \\ & \left. \int_{X_0}^{X_1}\int_{Z_0}^{Z_1}\int_0^{\infty} \nabla_{\tilde{\mathcal{S}}} J^H \delta\tilde{\mathcal{S}} \, h_1 h_2 h_3 \, dx^3 \, dx^2 \, dx^1 \right\}, \end{aligned} \tag{6}$$

where

$$\nabla_\xi J \, \delta\xi = \lim_{s\to 0} \frac{J(\xi + s\delta\xi) - J(\xi)}{s},$$

and $\delta\tilde{\mathbf{u}}_\mathrm{W}, \delta\tilde{T}_\mathrm{W}$ and $\delta\tilde{\mathcal{S}}$ are the variations of the input parameters. The gradient expressions, *i.e.* the sensitivities, are derived in appendix B, using a perturbation technique together with integration by parts in space. It yields

$$\begin{aligned}
\nabla_{\tilde{u}_\mathrm{W}} J &= \frac{\mu}{\bar{\Theta} R} D_3(u^*) && \text{on } x^3 = 0 \\
\nabla_{\tilde{v}_\mathrm{W}} J &= \frac{\mu}{\bar{\Theta} R} D_3(v^*) && \text{on } x^3 = 0 \\
\nabla_{\tilde{w}_\mathrm{W}} J &= \frac{\rho\rho^*}{\bar{\Theta}} && \text{on } x^3 = 0 \\
\nabla_{\tilde{T}_\mathrm{W}} J &= -\frac{\kappa}{\bar{\Theta}\,\mathrm{Pr}\,R} D_3(T^*) && \text{on } x^3 = 0 \\
\nabla_{\tilde{\mathcal{S}}} J &= \frac{\phi^*}{\bar{\Theta}} && \text{in } \Omega
\end{aligned} \tag{7}$$

where the overbar denotes the complex conjugate, μ, κ, R and Pr are the dynamic viscosity, the heat conductivity, the Reynolds and Prandtl numbers, respectively, and

$$D_i = \frac{1}{h_i}\frac{\partial}{\partial x^i}.$$

The co-state variables $\phi^* = (\rho^*, u^*, v^*, w^*, T^*)$ and r^* satisfy the adjoint equations

$$\begin{aligned} \hat{\mathcal{L}}^*\,\phi^* &= \mathcal{S}^* && \text{in } \Omega \\ \mathbf{u}^* = 0, \quad T^* &= 0 && \text{on } x^3 = 0 \\ \mathbf{u}^* \to 0, \quad T^* &\to 0 && \text{as } x^3 \to \infty \\ \phi^* = \phi_1^*, \quad r^* &= r_1^* && \text{on } x^1 = X_1 \\ \frac{\partial}{\partial x^1}\int_0^{+\infty} \phi^{*H}\frac{\partial \hat{\mathcal{L}}}{\partial \alpha}\,\hat{\phi}\,h_1h_2h_3\,dx^3 &= f^* && \forall\ x^1 \end{aligned} \tag{8}$$

where

$$\mathcal{S}^* = -\Big[\bar{r}^* D_1(\hat{\phi}) - D_1(r^*\hat{\phi}) - (m_{21}+m_{31})r^*\hat{\phi}\Big], \tag{9}$$

$$\begin{aligned} f^* = i\int_0^{+\infty} \phi^{*H}\hat{\mathcal{S}}\,h_1h_2h_3\,dx^3 + ih_1h_2\Big[-\frac{\kappa}{\mathrm{Pr}\,R}D_3(\bar{T}^*)\hat{T} \\ +(\rho\bar{\rho}^*)\hat{w} + \frac{\mu}{R}D_3(\bar{u}^*)\hat{u} + \frac{\mu}{R}D_3(\bar{v}^*)\hat{v}\Big]\Big|_{x^3=0}. \end{aligned} \tag{10}$$

and

$$m_{ij} = \frac{1}{h_ih_j}\frac{\partial h_i}{\partial x^j}.$$

The co-state equations (8) are integrated in the upstream direction with the initial condition at $x^1 = X_1$ as :

$$\phi_1^* = |\Theta_1|^2(\mathcal{D}^H)^{-1}(\mathcal{M} - c_1\mathcal{I})\hat{\phi}_1, \qquad r_1^* = |\Theta_1|^2\,c_1 \tag{11}$$

where c_1 is given in the appendix and $\mathcal{I}$ is the identity matrix. Equations (8) are solved iteratively to find r^* such that the integral expression is satisfied.

Now, the gradients of J can be obtained in following steps. First, the state variable ϕ is calculated by integrating equations (3) from $x^1 = X_0$ to X_1. Then the co-state equations (8) are integrated backward in the streamwise direction from $x^1 = X_1$ to X_0 to obtain the co-state variables ϕ^*. Finally, equations (7) give the gradients with respect to each control parameter.

It is worth mentioning that the expression for $\mathcal{S}^*$ depends on the choice of the auxiliary condition while the adjoint operator $\hat{\mathcal{L}}^*$ will remain unchanged for other choices of this condition. If the output is defined as in (2) the adjoint system will be

$$\begin{aligned} \hat{\mathcal{L}}^*\,\phi^* &= \mathcal{S}^* + \mathcal{M}^H\hat{\phi}|\Theta|^2 && \text{in } \Omega \\ \mathbf{u}^* = T^* &= 0 && \text{on } x^3 = 0 \\ \mathbf{u}^*,\, T^* &\to 0 && \text{as } x^3 \to \infty \\ \phi^* = r^* &= 0 && \text{on } x^1 = X_1 \end{aligned} \tag{12}$$

Table I. Spanwise wavenumber β with corresponding wave angle φ at $R = 160$ for different Mach numbers M. $F = 10^{-4}$

β		0	0.02	0.04
$M = 0,$	$\varphi =$	0°	22.3°	41.2°
$M = 0.7,$	$\varphi =$	0°	23.5°	42.5°
$M = 1.2,$	$\varphi =$	0°	25.9°	45.2°

$$\frac{\partial}{\partial x^1}\int_0^{+\infty} \phi^{*H}\frac{\partial \hat{\mathcal{L}}}{\partial \alpha}\,\hat{\phi}\,h_1h_2h_3dx^3 + |\Theta|^2\int_0^{+\infty}\hat{\phi}^H\mathcal{M}\hat{\phi}\,h_1h_2h_3\,dx^3 = f^*\forall x^1$$

Note that in this case both ϕ^* and r^* are subjected to homogeneous initial conditions.

4. Results

The results presented here are obtained by numerically integrating the discretized state and co-state equations. The x^1-derivatives are approximated by a first-order accurate backward Euler scheme and the x^3-derivatives by a fourth-order accurate compact finite-difference scheme. For details the reader is referred to Hanifi *et al.* (1994).

The calculations are performed for two- and three dimensional disturbances in a two-dimensional compressible boundary layer on an adiabatic flat plate. The gradients express the sensitivity of disturbances to small unsteady inhomgeneities in the steady boundary layer flow. The stagnation temperature is 300 K and the Prandtl number is held constant to $\mathrm{Pr} = 0.72$. The dynamic viscosity is calculated using Sutherland law and the coefficient of the specific heat c_p is assumed to be constant. The ratio of the coefficients of second and dynamic viscosity is given by the Stoke's hypothesis, *i.e.* $\lambda/\mu = -2/3$. In all figures the reduced frequency, defined as $F = 2\pi f^\star \nu_e^\star/U_e^{\star 2}$, is equal to 10^{-4}. Here $f^\star$ is the dimensional physical frequency and the subscript $_e$ refers to values at the edge of the boundary layer. The output is measured at $R = \sqrt{U_e^\star x^{1\star}/\nu_e^\star} = 760$. The calculations have been performed for three values of spanwise wavenumbers β at different Mach numbers. Values of the wave angle φ given at $x^1 = X_0$ for the cases studied here are given in table I. In all calculations, the metric coefficients $h_1 = h_2 = h_3 = 1$.

4.1. Accuracy of the gradient, validation

In order to verify the correctness of the gradient, we compare the adjoint based gradients to those obtained using the finite-difference approach. In the latter, the derivative of the output variable with respect to each input parameter is approximated by a second-order accurate central finite-difference scheme.

To compare the gradients given by the adjoint and finite-difference approaches let us consider the example of a wall normal velocity perturbation $\delta\tilde{w}_{\rm w}$ at $x^3 = 0$. The variation of a functional J with respect to this wall perturbation is :

$$\delta J = \frac{\partial J}{\partial \tilde{w}_r}\delta\tilde{w}_r + \frac{\partial J}{\partial \tilde{w}_i}\delta\tilde{w}_i \tag{13}$$

The subscripts $_r$ and $_i$ denote the real and imaginary parts of a complex number. In the finite-difference approach, the derivatives of J are obtained by imposing the inhomogeneous boundary condition $\tilde{w}_{\rm w} = \pm\varepsilon$ at $x^1 = x^1_n$. Here, ε is a small number and index n refers to n-th streamwise position. Then, the derivatives are calculated using a second-order accurate finite-difference scheme.

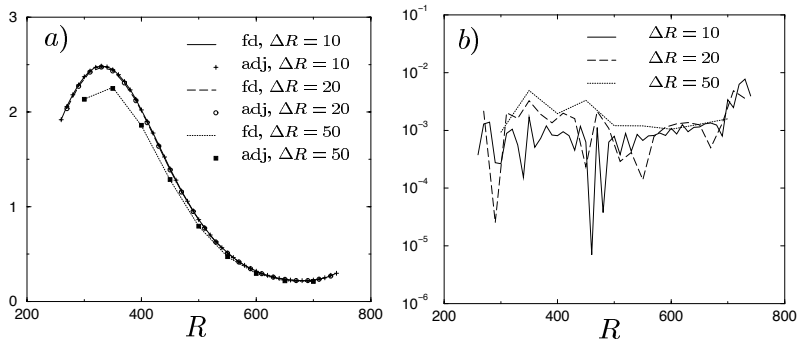

Figure 2. Comparison between adjoint (adj) and central difference (fd) calculations for different ΔR. Mach number $M = 0.7$, $\beta = 0$. a) lines denote $\|(\partial J/\partial\tilde{w}_r, \partial J/\partial\tilde{w}_i)/\Delta_n\|$ and symbols $|\nabla_{\tilde{w}_{\rm w}} J_n|$. b) relative error.

The expression for δJ in the adjoint approach, for a flat plate geometry, is in discretized form given as

$$\delta J = \int_{Z_0}^{Z_1} \sum_{n=2}^{N-1} \frac{1}{2}(\nabla_{\tilde{w}_{\rm w}} J^H_n \delta\tilde{w}_{{\rm w}n} + c.c.)\Delta_n \, dx^2, \tag{14}$$

where $\Delta_n = (x^1_{n+1} - x^1_{n-1})/2$ and $c.c.$ is the complex conjugate. In the following, the quantity $\nabla_{\tilde{w}_{\rm w}} J_n$ is compared to those of the finite-difference approach. The streamwise domain used here is $R \in [250, 750]$.

In figure 2a the modulus $||(\partial J/\partial \tilde{w}_r, \partial J/\partial \tilde{w}_i)/\Delta_n||$, as a function of x_n^1, is compared to $|\nabla_{\tilde{w}_w} J_n|$ for different resolution of the streamwise step ΔR. A good agreement is found between the approaches for a given ΔR, and both values converge as ΔR is decreased. The relative error given in figure 2b is below one percent for all cases and decreases slightly as ΔR is decreased.

The phase Φ of the gradients obtained by adjoint equations and central differences is compared in figure 3a for a given streamwise step, $\Delta R = 10$. The absolute error of the phase shown in figure 3b is less than 0.1 degrees except close to the outlet of the domain.

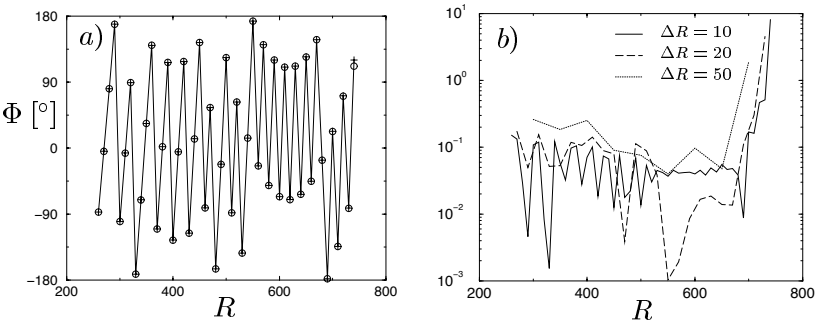

Figure 3. Comparison between adjoint and central difference calculations of the phase Φ in degrees for $M = 0.7$, $\beta = 0$. a) $\Delta R = 10$. + denotes central difference, and ∘ denotes adjoint calculations. b) absolute error in degrees.

4.2. Sensitivity to wall disturbances.

In figures 4, 5 and 6 the modulus of the gradient for inhomogeneous wall boundary conditions are shown for three different Mach numbers M and spanwise wavenumbers β. As can be seen in there, the maximum value of the gradient is achieved if forcing is situated close to branch I of the neutral stability curve. This is in agreement with receptivity studies of *e.g.* Hill (1995), Airiau, Walther and Bottaro (2001) and Airiau (2000). In Airiau *et al.* the wall gradients were interpreted as wall Green's functions. One should note that the distance between the maximum value of the gradient and Branch I of the neutral stability curve depends on the Mach number and the input parameter. Branch I and branch II are marked on each curve in the figures with + signs. For low Mach numbers, the two-dimensional waves, $\beta = 0$, give the largest value of the gradient for wall-disturbance components $\tilde{u}, \tilde{v}, \tilde{w}$ and $\tilde{T}$. This can be seen for $M = 0$ and $M = 0.7$ in figures 4 and 5, respectively. As is shown in figure 6, where $M = 1.2$, it is clear that for higher Mach numbers the two-dimensional waves do not have the largest gradient.

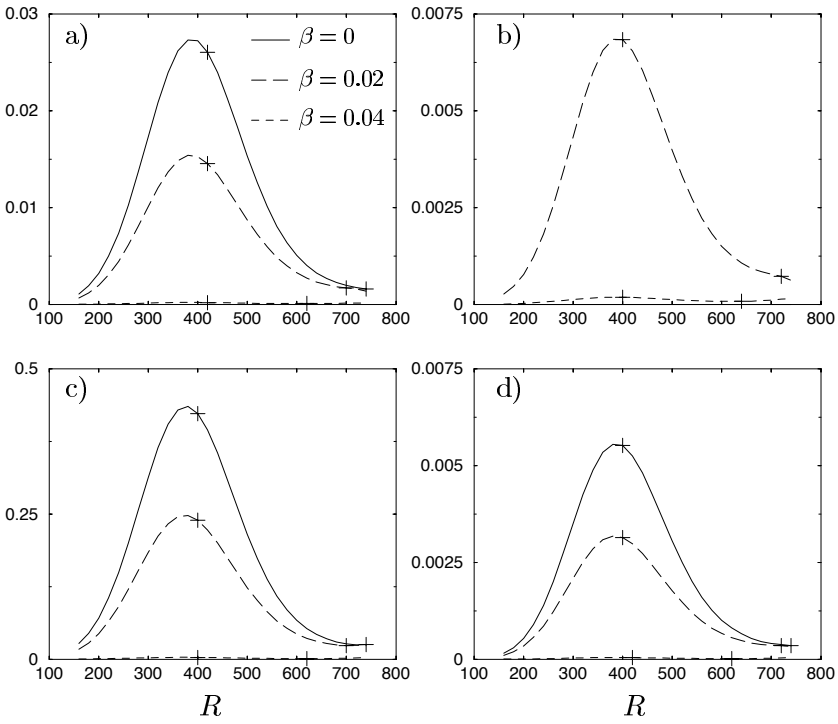

Figure 4. Modulus of the gradients due to 2D and 3D wall disturbances as a function of the Reynolds number for a Mach number $M = 0$. a) $|\nabla_{\tilde{u}_w} J|$, streamwise velocity component; b) $|\nabla_{\tilde{v}_w} J|$ spanwise velocity component; c) $|\nabla_{\tilde{w}_w} J|$ normal velocity component; d) $|\nabla_{\tilde{T}_w} J|$ temperature component.

This observation follows the fact that in compressible boundary layers the three-dimensional disturbances are the most unstable ones (see *e.g.* Mack 1984).

The magnitude of the gradient is quite different comparing $\tilde{u}, \tilde{v}, \tilde{w}$ and $\tilde{T}$ in figures 4, 5 and 6. It was noted that the normal velocity component gave the largest gradient for various spanwise wavenumber at Mach numbers between 0 and 1.2. The response to the wall normal velocity component was one order of magnitude larger than the streamwise and spanwise velocity components. In cases studied here, the normal component is about 15 times that of the streamwise component. This implies that blowing and suction at the wall is the most efficient mean of controlling the instability waves. However, as is shown in the figures, the maximum response to a wall disturbance decreases as the Mach number increases. This means that the efficiency

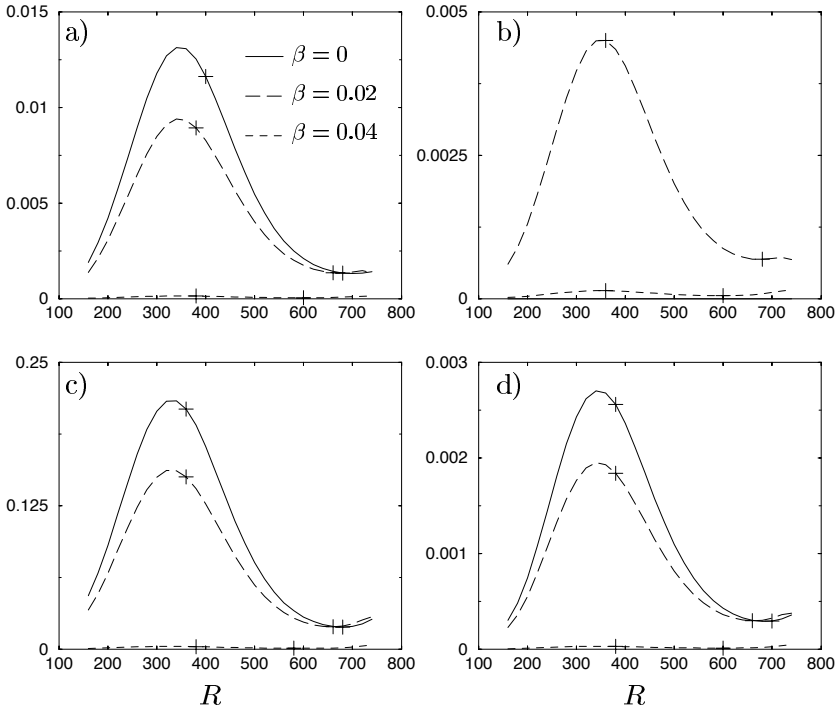

Figure 5. Modulus of the gradients due to 2D and 3D wall disturbances as a function of the Reynolds number for a Mach number $M = 0.7$. a) $|\nabla_{\tilde{u}_w} J|$, streamwise velocity component; b) $|\nabla_{\tilde{v}_w} J|$ spanwise velocity component; c) $|\nabla_{\tilde{w}_w} J|$ normal velocity component; d) $|\nabla_{\tilde{T}_w} J|$ temperature component.

of blowing and suction for control of disturbance growth decreases at higher Mach numbers.

4.3. Sensitivity to momentum sources.

In figure 7 the modulus of the gradients for the streamwise and normal momentum forcing are plotted. The Mach number and spanwise wavenumber are both zero in this case. However, the qualitative behavior does not change for higher Mach numbers up to 1.2, and spanwise wavenumbers of 0, 0.02 and 0.04 which were studied here. A first observation is that the gradient for the streamwise component of a source of momentum $|\nabla_{\tilde{\mathcal{S}}_u} J|$ is about 10 times that of the normal component. Further, the maximum value of $|\nabla_{\tilde{\mathcal{S}}_u} J|$ is located near branch I of the neutral stability curve. It was noted by *e.g.* Hill (1995) that forcing most effectively is done in the vicinity of the critical layer, *i.e.* where the streamwise velocity $U(x, y) = \omega / \texttt{Real}\{\alpha\}$. This was also found in

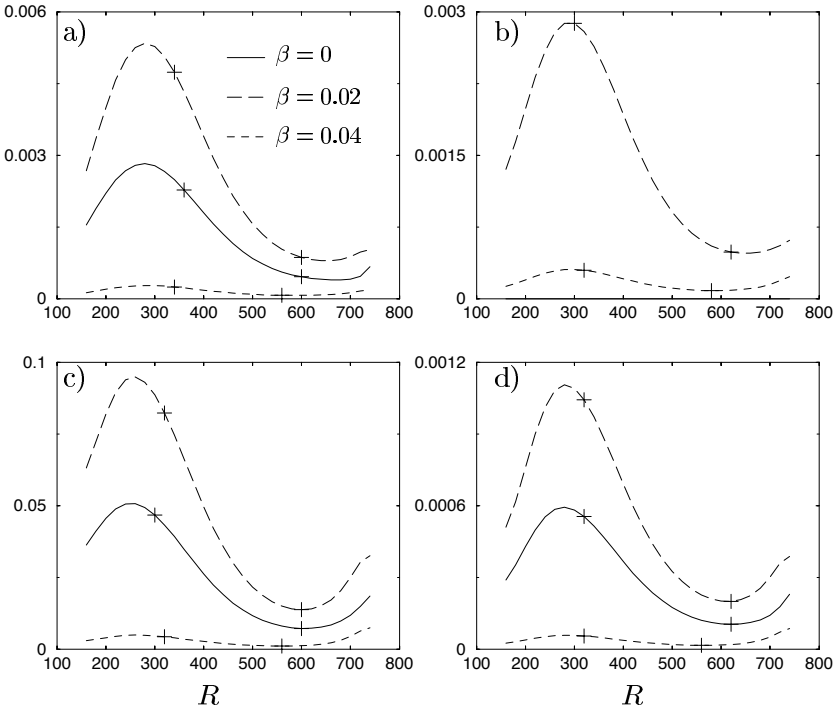

Figure 6. Modulus of the gradients due to 2D and 3D wall disturbances as a function of the Reynolds number for a Mach number $M = 1.2$. a) $|\nabla_{\tilde{u}_w} J|$, streamwise velocity component; b) $|\nabla_{\tilde{v}_w} J|$ spanwise velocity component; c) $|\nabla_{\tilde{w}_w} J|$ normal velocity component; d) $|\nabla_{\tilde{T}_w} J|$ temperature component.

our analysis. The location of the critical layer is marked with a line in figure 7a.

5. Conclusions

The Adjoint Parabolized Stability Equations (APSE) have been derived for quasi three-dimensional compressible flow using an input/output framework. The equations are given for an orthogonal curvilinear coordinate system. The adjoint field gives the sensitivity of disturbances to changes in boundary conditions and momentum forcing. These equations provide a basis for optimal control of disturbance growth using unsteady wall perturbation or unsteady momentum forcing.

In the present formulation, the sensitivity of the objective function (output) to all control parameters (input) is found by solving the

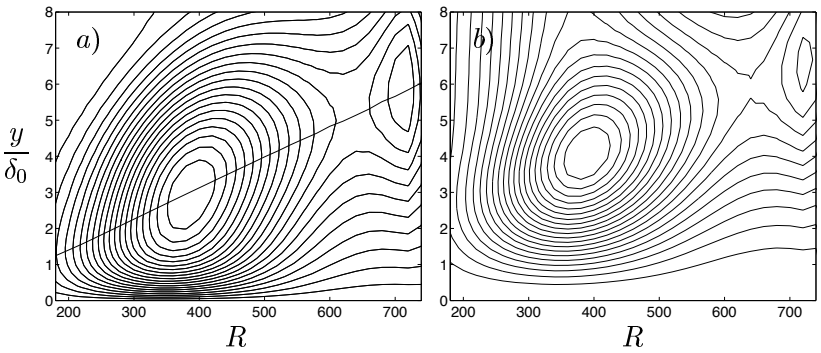

Figure 7. Contour plot of the gradients for momentum forcing. δ_0 denotes the boundary-layer thickness at streamwise position $x^1 = X_0$. $F = 10^{-4}$, $M = 0.7$, $\beta = 0$. The line in a) shows the position of the critical layer. a) $|\nabla_{\mathcal{S}_u} J|$, streamwise component with maximum = 1.8. Branch locations: I at $R \approx 400$, II at $R \approx 680$. b) $|\nabla_{\mathcal{S}_w} J|$, normal component with maximum = 0.16. Branch locations: I at $R \approx 360$, II at $R \approx 680$.

state equations and their adjoint once. This will drastically reduce the computational costs in an optimal design procedure.

The accuracy of the gradients have been verified by comparing the gradients derived by the adjoint equations with a finite-difference approach. It was shown that as the streamwise resolution is increased the differences between these two methods decrease and the solution of the gradient converges.

Analysis of two-dimensional boundary layers shows that a given disturbance is most sensitive to wall- and momentum forcing close to branch I of the neutral stability curve. The streamwise distance between the maximum of sensitivity and Branch I depends on the input component. This was found to be true for $0 \leqslant M \leqslant 1.2$ studied here. We also found that the response to the inhomogeneities of normal velocity at the wall is at least one order of magnitude larger than those of other the velocity components and temperature. This is in agreement with Hill (1995) for incompressible flow.

For incompressible flows, it has been shown that the two-dimensional disturbances are the most sensitive ones to wall inhomogeneity. However, for compressible flows, the three-dimensional disturbances are the most sensitive ones. Further, it has been observed that momentum forcing is most effectively done in the vicinity of the critical layer, which has earlier been shown by Hill for incompressible boundary layer.

The results shown here are obtained with an objective function solely defined by the terminal energy. If instead the disturbance energy over the entire domain is used then the peak of the gradient would probably

move another streamwise position. Further, if the cost of the control energy is added to the objective function as $J = E + \epsilon E_c$ then the results will most certainly change. One point that has to be made clear when adding the control energy is that the goal is not just to find the gradient for the disturbance energy but also for the control energy used. In the simple case shown in this article it turns out that the gradient appear to be similar to well known stability results, however what will happen in the other cases described above is left for future investigations.

Acknowledgements

The second author wishes to thank the 'Conférence des Grandes Ecoles' and FFA for their financial support. This work was carried out during a three-months period at FFA where he appreciated the Swedish friendship. The authors also wish to thank Martin Berggren at FFA for valuable discussions.

References

AIRIAU, C. 2000. 'Non-parallel acoustic receptivity of a Blasius boundary layer using an adjoint approach.' *in press in Flow, Turbulence and Combustion.*

AIRIAU, C., WALTHER, S., BOTTARO, A. 1999. 'Non-parallel receptivity and the adjoint PSE.' to appear in *IUTAM Symposium on Laminar-Turbulent Transition (September 1999, Sedona, AZ), Fasel, H. and Saric, W., eds. Springer.*

ANDERSSON, P., BERGGREN, M. AND HENNINGSON, D.S. 1999. 'Optimal disturbances and bypass transition in boundary layer.' *Phys. Fluids*, **11**, pp. 134–150.

ANDERSSON, P., HENNINGSON, D.S. AND HANIFI, A. 1998. 'On a stabilization procedure for the parabolic stability equations.' *J. Eng. Math.*, **33**, pp. 311–332.

BEWLEY, T.R., TEMAM, R. AND ZIANE, M. 2000. 'A general framework for robust control in fluid mechanics.' *Physica D*, **138**, pp. 360–392.

BERTOLOTTI, F.P., HERBERT, TH. AND SPALART, S.P. 1992. 'Linear and Nonlinear Stability of the Blasius Boundary Layer.' *J. Fluid Mech.*, **242**, pp. 441–474.

CATHALIFAUD, P. AND LUCHINI, P. 2000. 'Algebraic growth in a boundary layer: optimal control by blowing and suction at the wall.' *Eur. J. Mech. B/Fluids*, **19**(4), pp. 469–490

CHOUDHARI, M. AND STREET, C.L. 1992. 'A finite reynolds-number approach for the prediction of boundary-layer receptivity in localized regions.' *Phys. Fluids A*, **4**, pp. 2495–2514.

CORKE, T.C., BAR-SEVER, A. AND MORKOVIN, M.V. 1986. 'Experiments on transition enhancement by distributed roughness.' *Phys. Fluids.* **29**, pp. 3199–3213.

CROUCH, J.D. 1992a. 'Localized receptivity of boundary layers.' *Phys. Fluids A* **4**, pp. 1408–1414.

CROUCH, J.D. 1992b. 'Non-localized receptivity of boundary layers.' *J. Fluid Mech.* **244**, pp. 567–581.

GOLDSTEIN, M.E. 1983. 'The evolution of Tollmien-Schlichting waves near the leading edge.' *J. Fluid Mech.* **127**, pp. 59–81.

Goldstein, M.E. and Hultgren, L.S. 1989. 'Boundary-layer receptivity to long-wave free-stream disturbances.' *Ann. Rev. Fluid Mech.*, **21**, pp. 137–166.

GUNZBURGER, M. 2000. 'Adjoint equation-based methods for control problems in incompressible, viscous flows.' *in press in Flow, Turbulence and Combustion.*

HALL, M. C. G. 1986. 'Application of Adjoint Sensitivity Theory to an Atmospheric General Circulation Model.' *J. The Atmospheric Sci.* **43**, pp. 2644–2651.

HANIFI, A., HENNINGSON, D.S., HEIN, S., BERTOLOTTI, F.P. AND SIMEN, M. 1994. 'Linear Non-local Instability Analysis - the linear NOLOT code.' *FFA TN* 1994-54, See also Hein et al. 1994.

Hanifi, A. and Schmid, P.J., Henningson, D.S. 1996. 'Transient growth in compressible boundary layer flow' *Phys. Fluids* **8**(3), pp. 826–837.

HEIN, S., BERTOLOTTI, F.P., SIMEN, M., HANIFI, A. AND HENNINGSON, D.S. 1994. 'Linear Non-local Instability Analysis - the linear NOLOT code.' *DLR-IB* 223-94 A 43.

HERBERT, TH. 1994. 'Parabolized Stability Equations.' *AGARD Report* No. 793, pp. 4-1–4-34.

HILL, D. C. 1995. 'Adjoint Systems and their role in the Receptivity Problem for Boundary Layers.' *J. Fluid Mech.* **292**, pp. 183–204.

HILL, D. C. 1997. 'Receptivity in non-parallel boundary layers.' *ASME Fluids Engineering Division Summer Meeting, FEDSM '97, June 22-26, 1997.*

HÖGBERG, M. AND BERGGREN, M. 2000. 'Numerical approaches to optimal control of a model equation for shear flow instabilities. *, Submitted to Journal of Flow, Turbulence and Combustion.*

LI, F. AND MALIK, M.R. 1996 'On the Nature of PSE Approximation.' *Theoretical and Computational Fluid Dynamics* No.**8**, pp. 253–273.

LUCHINI, P. AND BOTTARO, A. 1998 'Görtler vortices : a backward-in-time approach to the receptivity problem.' *J. Fluid Mech.*, **363**, pp. 1–23.

LUCHINI, P. 2000 'Reynolds-number-independent instability of the boundarylayer over a flat surface: optimal perturbations.' *J. Fluid Mech.*, **404**, pp. 289–309.

MACK, L.M. 1984 'Boundary-layer stability theory.' *AGARD Report* No. 709, pp. 3-1–3-81.

NISHIOKA, M. AND MORKOVIN, M.V. 1986. 'Boundary-layer receptivity to unsteady pressure gradients : experiments and overview.' *J. Fluid Mech.* **171**, pp. 219–261.

PRALITS, J.O., HANIFI, A. AND HENNINGSON, D.S. 2000. 'Adjoint-based suction optimization for 3D boundary layer flows' *FFA TN* 2000-58.

SARIC, W.S. 1993. 'Physical description of boundary-layer transition : experimental evidence' *AGARD report* **793**, pp. 183–204.

SIMEN, M. 1992. 'Local and Nonlocal Stability Theory of Spatially Varying Flows.' *Instability, Transition and Turbulence*, Springer Verlag, pp. 181–201

THOMAS, A. 1983. 'The control of boundary-layer transition using a wave superposition principle.' *J. Fluid Mech.* **137**, pp.233–250.

TUMIN, A. 1996. 'Receptivity of Pipe Poiseuille Flow.' *J Fluid Mech.* **315**, pp. 119–137.

Appendix

A. The non-local stability equations

A.1. Governing equations and assumptions

A model of convectively unstable waves with curved or divergent wave-rays in a non-uniform flow is described here. The equations are derived from the equations of conservation of mass, momentum and energy and the equation of state governing the flow of a viscous, compressible, ideal gas expressed in primitive variables and curvilinear coordinates. The non-dimensional conservation equations in vector notation are given by

$$\rho\,[\frac{\partial \mathbf{u}}{\partial t}+(\mathbf{u}\cdot\nabla)\mathbf{u}] = -\nabla p+\frac{1}{R}\nabla[\lambda(\nabla\cdot\mathbf{u})]+\frac{1}{R}\nabla\cdot[\mu(\nabla\mathbf{u}+\nabla\mathbf{u}^T)], \quad (15)$$

$$\frac{\partial \rho}{\partial t}+\nabla\cdot(\rho\mathbf{u}) = 0, \quad (16)$$

$$\rho c_p[\frac{\partial T}{\partial t}+(\mathbf{u}\cdot\nabla)T] = \frac{1}{R\,\mathrm{Pr}}\nabla\cdot(\kappa\nabla T)+(\gamma-1)M^2[\frac{\partial p}{\partial t}+(\mathbf{u}\cdot\nabla)p+\frac{1}{R}\Phi], \quad (17)$$

$$\gamma M^2 p = \rho T, \quad (18)$$

with viscous dissipation given as

$$\Phi = \lambda(\nabla\cdot\mathbf{u})^2+\frac{1}{2}\mu[\nabla\mathbf{u}+\nabla\mathbf{u}^T]^2.$$

Here t represents time, ρ, p, T stand for density, pressure and temperature, $\mathbf{u}$ is the velocity vector. The quantities λ, μ stand for the second and dynamic viscosity coefficient, γ is the ratio of specific heats, κ the heat conductivity, c_p the specific heat at constant pressure. All flow quantities are made non-dimensional by corresponding reference flow quantities at a fixed streamwise position $x_0^\star$, except the pressure which is referred to twice the corresponding dynamic pressure. The reference length scale is fixed and taken as

$$l_0^\star = \sqrt{\frac{\nu_0^\star x_0^\star}{U_0^\star}}.$$

The Mach number, M, Prandtl number, Pr and Reynolds number, R are defined as

$$M = \frac{U_0^\star}{\sqrt{\Re\gamma T_0^\star}}, \quad \mathrm{Pr} = \frac{\mu_0^\star c_{p0}^\star}{\kappa_0^\star}, \quad R = \frac{U_0^\star l_0^\star}{\nu_0^\star},$$

where $\Re$ is the specific heat constant and superscript * refers to dimensional quantities.

We decompose the flow and material quantities into a mean flow part Q and a disturbance $\tilde{q}$ as $Q_{tot}(x^i,t) = Q(x^i) + \tilde{q}(x^i,t)$ where x^1, x^2 and x^3 are the normal, spanwise and streamwise components respectively. Here $Q \in [U,V,W,p,T,\rho]$ and $\tilde{q} \in [\tilde{u},\tilde{v},\tilde{w},\tilde{p},\tilde{T},\tilde{\rho}]$, where U,V,W are the streamwise, spanwise and normal components of the mean velocity vector, respectively. u,v,w are those of the perturbation velocity vector. The domain considered is defined as $x^1 \in [X_0,X_1]$, $x^2 \in [Z_0,Z_1]$ and $x^3 \in [0,\infty[$. To simplify the analysis the mean flow is considered to be independent of the spanwise coordinate x^2. Two assumptions are made to derive the non-local stability equations. The first is of WKB type where the disturbance $\tilde{q}$ is divided into an amplitude function and a wave function

$$\tilde{q}(x^i,t) = \hat{q}(x^1,x^3)\Theta, \quad \Theta = \exp\ i\,(\int_{X_0}^{x^1} \alpha(x')dx' + \beta x^2 - \omega t).$$

Here α is a complex wavenumber, β the real spanwise wavenumber and ω the real angular wave frequency. The second assumption is a scale separation $1/R$ between the weak variation in the x^1 direction and the strong variation in the x^3 direction analogous to the multiple scales method. We assume

$$\frac{\partial}{\partial x^1} \sim \mathcal{O}(R^{-1}), \quad V \sim \mathcal{O}(R^{-1})$$

Furthermore, it is assumed that the metrics are of order $\mathcal{O}(R^{-1})$.

A.2. The linear non-local stability equations

The non-local stability equations are derived using Parabolized Stability Equation approach (PSE). We consider a general case where the boundary layer is subjected to sources of mass, momenta and energy, $\tilde{\mathcal{S}}$, and inhomogeneous boundary conditions on the wall. The linearized disturbance equations are obtained by introducing the variable decomposition into the governing equations (15)-(18), subtracting the equations for the mean flow and removing the products of disturbances. We proceed with the derivation of the stability equations by introducing the scaling relations given in section A.1. Finally, collecting terms up to order $\mathcal{O}(R^{-1})$ gives a set of nearly parabolic partial differential equations. A note on the parabolic nature of PSE can be found in *e.g.* Li and Malik (1996), and Andersson, Henningson and Hanifi (1998). The equation can now be written

$$\hat{\mathcal{L}}\,\hat{\phi}(x^1,x^3) = \hat{\mathcal{S}}(x^1,x^3) \tag{19}$$

where the vector of the amplitude functions is $\hat{\phi} = (\hat{\rho}, \hat{u}, \hat{v}, \hat{w}, \hat{T})^{\mathrm{T}}$. The boundary conditions are

$$\begin{array}{ll} \hat{\mathbf{u}}(x^1,0) = \hat{\mathbf{u}}_{\mathrm{w}}(x^1), & \hat{T}(x^1,0) = \hat{T}_{\mathrm{w}}(x^1), \\ \lim\limits_{x^3\to\infty} \hat{\mathbf{u}} = 0 \quad \text{and} & \lim\limits_{x^3\to\infty} \hat{T} = 0. \end{array} \tag{20}$$

The operator $\hat{\mathcal{L}}$ is defined as

$$\hat{\mathcal{L}} = \mathcal{A} + \mathcal{B}D_3 + \mathcal{C}D_{33} + \mathcal{D}D_1 \tag{21}$$

where

$$D_i = \frac{1}{h_i}\frac{\partial}{\partial x^i}, \qquad D_{ii} = \frac{1}{h_i^2}\frac{\partial^2}{(\partial x^i)^2}.$$

Here, h_i is the scale factor such that a length element is defined as $ds^2 = (h_1 dx^1)^2 + (h_2 dx^2)^2 + (h_3 dx^3)^2$. The coefficients of the 5×5 matrices $\mathcal{A}$, $\mathcal{B}$, $\mathcal{C}$ and $\mathcal{D}$ can be found in appendix C. Furthermore, as both the amplitude function and the wave function depend on the x^1 coordinate, this ambiguity is removed by specifying an auxiliary condition

$$\int_0^\infty \hat{\phi}^H \frac{\partial \hat{\phi}}{\partial x^1}\, h_2 h_3 dx^3 = 0, \tag{22}$$

where, superscript ^{H} denotes the transpose complex conjugate. This condition also guarantees that x^1-variation of the disturbance amplitude function remains small such that second streamwise derivatives are negligible.

B. Derivation of the gradient

The gradients are derived using the adjoint equations of the Parabolized Stability Equations. A discrete or a continuous formulation may be used. It was concluded by Högberg *et al.* (2000) that a continuous formulation is a good enough approximation if control is performed on a problem with a dominating instability. This type of analysis can be done with the PSE therefore a continuous approach is used in this paper.

B.1. Inner product

For a compact notation of the adjoint equations, we will use the *formal adjoint* $\mathcal{L}^*$ of the differential operator $\mathcal{L}$ defined by the relation

$$(\mathcal{L}^*\Psi^*, \Phi) = (\Psi^*, \mathcal{L}\Phi) + \text{ boundary terms},$$

where the inner product $(\cdot,\cdot)$ is defined as

$$(\Phi,\Psi^*)=\int_{X_0}^{X_1}\int_{Z_0}^{Z_1}\int_0^{+\infty}\Phi^H\Psi^*\,h_1h_2h_3\,dx^3\,dx^2\,dx^1, \tag{23}$$

for $\mathbb{C}^n$-valued functions Φ and Ψ^*. Here, the superscript * stands for adjoint quantities.

B.2. Derivation of adjoint equations

At first, the equations (1), (19), (20) and (22) has to be differentiated with respect to the input variables $\hat{\mathbf{u}}_{\mathrm{w}},\hat{T}_{\mathrm{w}},\hat{\mathcal{S}}$ and the state variables α and ϕ

$$\begin{aligned}\delta J \;=\; \mathtt{Real}\Big\{&\int_{Z_0}^{Z_1}\int_0^{\infty}|\Theta_1|^2\hat{\phi}_1^H\mathcal{M}\delta\hat{\phi}_1h_2h_3\,dx^3\,dx^2\;+\\ &\int_{Z_0}^{Z_1}\int_0^{\infty}|\Theta_1|^2\hat{\phi}_1^H\mathcal{M}\hat{\phi}_1\;i\int_{X_0}^{X_1}\delta\alpha dx'\,h_2h_3\,dx^3\,dx^2\Big\}\end{aligned} \tag{24}$$

$$\begin{aligned}\hat{\mathcal{L}}\,\delta\hat{\phi}-\delta\hat{\mathcal{S}}+\frac{\partial\hat{\mathcal{L}}}{\partial\alpha}\delta\alpha\,\hat{\phi} \;&=\; 0 && \text{in } \Omega\\ \delta\phi_0 \;&=\; 0 && \text{on } x^1=X_0\\ \delta\hat{\mathbf{u}}(x^1,0) \;&=\; \delta\hat{\mathbf{u}}_{\mathrm{w}}(x^1) && \text{on } x^3=0\\ \delta\hat{\mathbf{u}} \;&\to\; 0 && \text{as } x^3\to\infty\\ \delta\hat{T}(x^1,0) \;&=\; \delta\hat{T}_{\mathrm{w}}(x^1) && \text{on } x^3=0\\ \delta\hat{T} \;&\to\; 0 && \text{as } x^3\to\infty\\ \int_0^{\infty}(\delta\hat{\phi}^H\frac{\partial\hat{\phi}}{\partial x^1}+\hat{\phi}^H\frac{\partial\delta\hat{\phi}}{\partial x^1})\,h_2h_3dx^3 \;&=\; 0 && \forall\; x^1\end{aligned} \tag{25}$$

Note here that the variation of a disturbance ϕ results in the variation of both the amplitude function $\hat{\phi}$ and the streamwise wave-number α. A complex co-state vector $\phi^*=(\rho^*,u^*,v^*,w^*,T^*)^{\mathrm{T}}$ and complex function $r^*(x^1)$ are introduced. The adjoint equations are derived by taking the inner product of vector ϕ^* with the differentiated state equations, and r^* with the differentiated auxiliary condition according to the inner product (23). The complex conjugate of each term in the equation is added. Then, derivatives are removed from the differentiated variables in equation (26) using integration by parts. After integrations, it yields (without complex conjugate for clarity)

$$(\phi^*,\;\hat{\mathcal{L}}\,\delta\hat{\phi}-\delta\hat{\mathcal{S}}+\frac{\partial\hat{\mathcal{L}}}{\partial\alpha}\delta\alpha\,\hat{\phi})+$$

$$\int_{X_0}^{X_1}\int_{Z_0}^{Z_1}\bar{r}^*\int_0^{+\infty}[\delta\hat{\phi}^H D_1(\hat{\phi})+\hat{\phi}^H D_1(\delta\hat{\phi})]\,h_1h_2h_3dx^3\,dx^2\,dx^1 =$$
$$(\hat{\mathcal{L}}^*\phi^*,\delta\hat{\phi})-(\phi^*,\delta\hat{\mathcal{S}})-$$
$$\int_{X_0}^{X_1}\int_{Z_0}^{Z_1}\int_0^{+\infty}\frac{\partial}{\partial x^1}(\phi^{*H}\frac{\partial\hat{\mathcal{L}}}{\partial\alpha}\,\hat{\phi}\,h_1h_2h_3)\int_{X_0}^{x^1}\delta\alpha dx'\,dx^3\,dx^2\,dx^1+$$
$$\int_{Z_0}^{Z_1}\int_0^{+\infty}\Big[\phi^{*H}\frac{\partial\hat{\mathcal{L}}}{\partial\alpha}\,\hat{\phi}\,h_1h_2h_3\int_{X_0}^{x^1}\delta\alpha dx'\Big]_{X_0}^{X_1}dx^3\,dx^2+$$
$$\int_{Z_0}^{Z_1}\int_0^{+\infty}\Big[\phi^{*H}\,\mathcal{D}\,\delta\hat{\phi}\,h_2h_3\Big]_{X_0}^{X_1}dx^3\,dx^2+$$
$$\int_{Z_0}^{Z_1}\int_{X_0}^{X_1}\Big[\Big\{\phi^{*H}\Big(\mathcal{B}-(m_{13}+m_{23}-m_{33})\,\mathcal{C}-D_3(\mathcal{C})\Big)\,\delta\hat{\phi}+$$
$$-D_3(\phi^{*H})\,\mathcal{C}\,\delta\hat{\phi}+\phi^{*H}\,\mathcal{C}\,D_3(\delta\hat{\phi})\Big\}\,h_1h_2\,dx^2\,dx^1\Big]_0^{\infty}+$$
$$\int_{X_0}^{X_1}\int_{Z_0}^{Z_1}\int_0^{+\infty}\Big(r^*D_1(\hat{\phi}^H)-D_1(\bar{r}^*\hat{\phi}^H)-$$
$$(m_{21}+m_{31})\bar{r}^*\hat{\phi}^H\Big)\,\delta\hat{\phi}\,h_1h_2h_3dx^3\,dx^2\,dx^1+$$
$$\int_{Z_0}^{Z_1}\int_0^{+\infty}\Big[h_2h_3\bar{r}^*\hat{\phi}^H\delta\hat{\phi}\Big]_{X_0}^{X_1}dx^3\,dx^2=0 \qquad (26)$$

where

$$m_{ij}=\frac{1}{h_ih_j}\frac{\partial h_i}{\partial x^j}.$$

Terms of $\delta\alpha$ have also been integrated in equation (26) in order to identify from δJ the boundary terms at X_1. Collecting terms of $\delta\hat{\phi}$ leads to the adjoint equations

$$\hat{\mathcal{L}}^*\phi^*=-\Big[\bar{r}^*D_1(\hat{\phi})-D_1(r^*\hat{\phi})-(m_{21}+m_{31})\,r^*\hat{\phi}\Big] \qquad (27)$$

In order to remove the terms of $\delta\hat{\phi}$ in the equation (26) as $x^3\to\infty$, the following homogeneous boundary conditions are chosen

$$\begin{array}{lllll}\mathbf{u}^*(x^1,0) &=& 0 & \text{and} & T^*(x^1,0) = 0,\\ \lim\limits_{x^3\to\infty}\mathbf{u}^* &=& 0 & \text{and} & \lim\limits_{x^3\to\infty}T^* = 0,\end{array} \qquad (28)$$

where $\mathbf{u}^*=(u^*,v^*,w^*)^{\mathrm{T}}$. Using the operator matrices of the forward problem, the adjoint operator $\hat{\mathcal{L}}^*$ can be identified

$$\hat{\mathcal{L}}^* = \tilde{\mathcal{A}}+\tilde{\mathcal{B}}\,D_3.+\tilde{\mathcal{C}}\,D_{33}.+\tilde{\mathcal{D}}\,D_1. \qquad (29)$$

where $\tilde{\mathcal{A}}, \tilde{\mathcal{B}}, \tilde{\mathcal{C}}$ and $\tilde{\mathcal{D}}$ are

$$\begin{aligned}
\tilde{\mathcal{A}} &= \mathcal{A}^H - D_3(\mathcal{B}^H) - (m_{13}+m_{23})\,\mathcal{B}^H + D_{33}(\mathcal{C}^H) \\
&\quad + 2\,(m_{13}+m_{23}-m_{33})\,D_3(\mathcal{C}^H) \\
&\quad - D_1(\mathcal{D}^H) - (m_{21}+m_{31})\,\mathcal{D}^H \\
\tilde{\mathcal{B}} &= -\mathcal{B}^H + 2\,D_3(\mathcal{C}^H) + 2\,(m_{13}+m_{23}-m_{33})\,\mathcal{C}^H \\
\tilde{\mathcal{C}} &= \mathcal{C}^H \\
\tilde{\mathcal{D}} &= -\mathcal{D}^H,
\end{aligned}$$

The system of equations (27) with corresponding boundary conditions (28) is parabolic in the streamwise direction and must be integrated upstream, from X_1 to X_0. The initial condition at X_1 is found by identifying δJ, equation (24), with the terms defined at X_1 in equation (26). Matching terms of $\delta\hat{\phi}$, and $\delta\alpha$ gives the following system of equations to solve for the initial condition for ϕ^* and r^*

$$\begin{aligned}
|\Theta_1|^2 \int_0^\infty \hat{\phi}_1^H \mathcal{M}\delta\hat{\phi}_1 h_2 h_3\, dx^3 &= \int_0^{+\infty} (\phi^{*H}\,\mathcal{D} + \bar{r}^*\hat{\phi}^H)\,\delta\hat{\phi}\, h_2 h_3 dx^3\Big|_{X_1} \\
i|\Theta_1|^2 \int_0^\infty \hat{\phi}_1^H \mathcal{M}\hat{\phi}_1 h_2 h_3\, dx^3 &= \int_0^{+\infty} \phi^{*H}\frac{\partial\hat{\mathcal{L}}}{\partial\alpha}\,\hat{\phi}\, h_1 h_2 h_3\, dx^3\Big|_{X_1}
\end{aligned} \tag{30}$$

Solving the above equations gives the initial condition for the adjoint equations at X_1 as

$$\begin{aligned}
\phi_1^* &= |\Theta_1|^2 \mathcal{D}^+(\mathcal{M} - c_1\mathcal{I})\hat{\phi}_1, \qquad r_1^* = |\Theta_1|^2\, c_1, \\
\bar{c}_1 &= \frac{\displaystyle\int_0^\infty (h_1\hat{\phi}_1^H\mathcal{M}\,\mathcal{D}^{+H}\frac{\partial\hat{\mathcal{L}}}{\partial\alpha}\hat{\phi}_1 - i\hat{\phi}_1^H\mathcal{M}\hat{\phi}_1)\, h_2 h_3\, dx^3}{\displaystyle\int_0^\infty \hat{\phi}_1^H\mathcal{D}^{+H}\frac{\partial\hat{\mathcal{L}}}{\partial\alpha}\hat{\phi}_1\, h_1 h_2 h_3\, dx^3},
\end{aligned} \tag{31}$$

where $\mathcal{D}^+ = (\mathcal{D}^H)^{-1}$. Since by definition $\delta\phi = 0$ at X_0, the remaining terms of equation (26) together with equation (24) can be written

$$\begin{aligned}
\delta J = \mathtt{Real}\Bigg\{ &\int_{X_0}^{X_1}\int_{Z_0}^{Z_1}\int_0^{+\infty} \phi^{*H}\delta\hat{\mathcal{S}}\, h_1 h_2 h_3\, dx^3\, dx^2\, dx^1 + \\
&\int_{X_0}^{X_1}\int_{Z_0}^{Z_1}\int_0^{+\infty} \frac{\partial}{\partial x^1}(\phi^{*H}\frac{\partial\hat{\mathcal{L}}}{\partial\alpha}\,\hat{\phi}\, h_1 h_2 h_3)\int_{X_0}^{x^1}\delta\alpha dx'\, dx^3\, dx^2\, dx^1 + \\
&\int_{Z_0}^{Z_1}\int_{X_0}^{X_1}\Big\{\phi^{*H}\Big[\mathcal{B} - (m_{13}+m_{23}-m_{33})\,\mathcal{C} - D_3(\mathcal{C})\Big]\,\delta\hat{\phi} + \\
&\qquad -D_3(\phi^{*H})\,\mathcal{C}\,\delta\hat{\phi} + \phi^{*H}\,\mathcal{C}\,D_3(\delta\hat{\phi})\Big\}\, h_1 h_2\, dx^2\, dx^1\Big|_{x^3=0}\Bigg\}
\end{aligned} \tag{32}$$

The gradient should be identified from the variation of $\tilde{\phi}$ and of $\tilde{\mathcal{S}}$. However in equation (32) the variation of the momentum source and wall boundary condition is expressed in terms of $\hat{\phi}$ and $\hat{\mathcal{S}}$. The total variation of $\tilde{\phi}$ and $\tilde{\mathcal{S}}$ is written

$$\delta\tilde{\phi} = \delta\hat{\phi}\,\Theta + \tilde{\phi}\,i\int_{X_0}^{x^1}\delta\alpha dx'\,, \qquad \delta\tilde{\mathcal{S}} = \delta\hat{\mathcal{S}}\,\Theta + \tilde{\mathcal{S}}\,i\int_{X_0}^{x^1}\delta\alpha dx' \tag{33}$$

From equation (33), $\delta\hat{\phi}$ and $\delta\hat{\mathcal{S}}$ are substituted into equation (32). The variation of the functional δJ with respect to the total variation of $\tilde{\phi}$ and $\tilde{\mathcal{S}}$ is now written

$$\begin{aligned}
\delta J = \texttt{Real}\Bigg\{ & \int_{X_0}^{X_1}\int_{Z_0}^{Z_1}\int_0^{+\infty}\frac{1}{\Theta}\phi^{*H}\delta\tilde{\mathcal{S}}\,h_1h_2h_3\,dx^3\,dx^2\,dx^1 + \\
& \int_{X_0}^{X_1}\int_{Z_0}^{Z_1} h_1h_2\Big[-\frac{\kappa}{\Theta\,\mathrm{Pr}\,R}D_3(\bar{T}^*)\delta T + \frac{(\rho\bar{\rho}^*)}{\Theta}\delta\tilde{w} + \\
& \qquad \frac{\mu}{\Theta R}D_3(\bar{u}^*)\delta\tilde{u} + \frac{\mu}{\Theta R}D_3(\bar{v}^*)\delta\tilde{v}\Big]\,dx^2\,dx^1\Big|_{x^3=0} - \\
& \int_{X_0}^{X_1}\int_{Z_0}^{Z_1}\int_0^{+\infty}\frac{\partial}{\partial x^1}(\phi^{*H}\frac{\partial\hat{\mathcal{L}}}{\partial\alpha}\,\hat{\phi}\,h_1h_2h_3)\int_{X_0}^{x^1}\delta\alpha dx'\,dx^3\,dx^2\,dx^1 + \\
& \int_{X_0}^{X_1}\int_{Z_0}^{Z_1}\int_0^{+\infty}\phi^{*H}\hat{\mathcal{S}}\,h_1h_2h_3\,i\int_{X_0}^{x^1}\delta\alpha dx' dx^3\,dx^2\,dx^1 + \\
& \int_{X_0}^{X_1}\int_{Z_0}^{Z_1} h_1h_2\Big[-\frac{\kappa}{\mathrm{Pr}\,R}D_3(\bar{T}^*)\hat{T} + (\rho\bar{\rho}^*)\hat{w} + \frac{\mu}{R}D_3(\bar{u}^*)\hat{u} + \\
& \qquad \frac{\mu}{R}D_3(\bar{v}^*)\hat{v}\Big]\,i\int_{X_0}^{x^1}\delta\alpha dx'\,dx^2\,dx^1\Big|_{x^3=0}\Bigg\}
\end{aligned} \tag{34}$$

In equation (34) the expression for the wall boundary terms have been expanded to clarify the dependence between each state variable and the adjoint quantities. In the derivation of the adjoint equations the co-state variable $r^*(x)$ has been used in order to incorporate the auxiliary condition. However, equation (27) gives a system with five equations and six co-state variables. Therefore, an additional equation is needed to close the system. Collecting the terms of $\delta\alpha$ in equation (34) provides an additional equation which must be satisfied for each position in x^1

$$\begin{aligned}
& \int_0^{+\infty}\frac{\partial}{\partial x^1}(\phi^{*H}\frac{\partial\hat{\mathcal{L}}}{\partial\alpha}\,\hat{\phi}\,h_1h_2h_3)\,dx^3 = i\int_0^{+\infty}\phi^{*H}\hat{\mathcal{S}}\,h_1h_2h_3\,dx^3 + \\
& i\,h_1h_2\Big[-\frac{\kappa}{\mathrm{Pr}\,R}D_3(\bar{T}^*)\hat{T} + (\rho\bar{\rho}^*)\hat{w} + \frac{\mu}{R}D_3(\bar{u}^*)\hat{u} + \frac{\mu}{R}D_3(\bar{v}^*)\hat{v}\Big]\Big|_{x^3=0}
\end{aligned} \tag{35}$$

It is denoted 'adjoint auxiliary condition' and is solved with an iterative process for r^* in a similar manner that equation (22) is solved for the streamwise wavenumber α. The gradient of the functional ∇J, with respect to the momentum forcing and wall disturbances can now be identified from the remaining terms of equation (34) as

$$\begin{aligned}
\nabla_{\tilde{u}_\mathrm{w}} J &= \frac{\mu}{\bar{\Theta} R} D_3(u^*) && \text{on } x^3 = 0 \\
\nabla_{\tilde{v}_\mathrm{w}} J &= \frac{\mu}{\bar{\Theta} R} D_3(v^*) && \text{on } x^3 = 0 \\
\nabla_{\tilde{w}_\mathrm{w}} J &= \frac{\rho \rho^*}{\bar{\Theta}} && \text{on } x^3 = 0 \\
\nabla_{\tilde{T}_\mathrm{w}} J &= -\frac{\kappa}{\bar{\Theta}\,\mathrm{Pr}\, R} D_3(T^*) && \text{on } x^3 = 0 \\
\nabla_{\tilde{\mathcal{S}}} J &= \frac{\phi^*}{\bar{\Theta}} && \text{in } \Omega
\end{aligned} \tag{36}$$

C. Operator matrices

The non-zero components of matrices $\mathcal{A}, \mathcal{B}, \mathcal{C}$ and $\mathcal{D}$ in equation (21) are

$$\begin{aligned}
a(1,1) &= U(m_{31} + m_{21}) + D_3(W) + D_1(U) + i\xi \\
a(1,2) &= \rho(i\alpha_0 + m_{31} + m_{21}) + D_1(\rho) \\
a(1,3) &= i\beta_0 \rho \\
a(1,4) &= \rho(m_{13} + m_{23}) + D_3(\rho) \\
a(2,1) &= \frac{1}{\gamma M^2}(D_1(T) + i\alpha_0 T) + D_1(U)U + D_3(U)W - m_{21}V^2 \\
a(2,2) &= \rho(D_1(U) + i\xi) + \frac{\mu}{R}(\alpha_0^2 l_2 + \beta_0^2) \\
a(2,3) &= -2\rho m_{21} V + \frac{\mu}{R}\alpha_0 \beta_0 l_1 \\
a(2,4) &= \rho(m_{13} U + D_3(U)) - \frac{i\alpha_0}{R}\frac{d\mu}{dT} D_3(T) \\
a(2,5) &= \frac{1}{\gamma M^2}(D_1(\rho) + i\rho\alpha_0) + \frac{1}{R}(-\frac{d\mu}{dT} D_{33}(U) - \\
&\quad D_3(U)\frac{d^2\mu}{dT^2} D_3(T)) \\
a(3,1) &= U(m_{21} V + D_1(V)) + D_3(V)W + \frac{i\beta_0}{\gamma M^2} T
\end{aligned}$$

$$
\begin{aligned}
a(3,2) &= \rho(m_{21}V + D_1(V)) + \frac{\mu}{R}\alpha_0\beta_0 l_1 \\
a(3,3) &= \rho(m_{21}U + i\xi) + \frac{\mu}{R}(\beta_0^2 l_2 + \alpha_0^2) \\
a(3,4) &= \rho(m_{23}V + D_3(V)) - \frac{i\beta_0}{R}\frac{d\mu}{dT}D_3(T) \\
a(3,5) &= \frac{i\beta_0}{\gamma M^2}\rho + \frac{1}{R}(-\frac{d\mu}{dT}D_{33}(V) - D_3(V)\frac{d^2\mu}{dT^2}D_3(T)) \\
a(4,1) &= \frac{1}{\gamma M^2}D_3(T) - m_{13}U^2 - m_{23}V^2 + \frac{i\mu}{R}\frac{l_2}{\rho}(\beta_0 D_3(V) + \\
&\quad \alpha_0 D_3(U)) \\
a(4,2) &= -2\rho m_{13}U - \frac{i\alpha_0}{R}l_0\frac{d\mu}{dT}D_3(T) + \frac{D_3(\rho)}{\rho}\frac{i\alpha_0}{R}\mu l_2 \\
a(4,3) &= -2\rho m_{23}V - \frac{i\beta_0}{R}l_0\frac{d\mu}{dT}D_3(T) + \frac{D_3(\rho)}{\rho}\frac{i\beta_0}{R}\mu l_2 \\
a(4,4) &= \rho(D_3(W) + m_{31}U + i\xi) + \frac{1}{R}\mu(\beta_0^2 + \alpha_0^2) + \\
&\quad \frac{D_{33}(\rho)}{\rho}\frac{\mu}{R}l_2 \\
a(4,5) &= \frac{1}{\gamma M^2}D_3(\rho) + \frac{1}{R}\frac{d\mu}{dT}i(-\beta_0 D_3(V) - D_3(U)\alpha_0) \\
a(5,1) &= \frac{(\gamma-1)}{\gamma}(UD_1(T) + WD_3(T) + iT\xi) + \\
&\quad c_p(-WD_3(T) - UD_1(T)) \\
a(5,2) &= (\gamma-1)M^2 D_1(p) - \rho c_p D_1(T) \\
a(5,4) &= (\gamma-1)M^2\left[D_3(p) + \frac{2i\mu}{R}(\beta_0 D_3(V) + D_3(U)\alpha_0)\right] - \rho c_p D_3(T) \\
a(5,5) &= \rho\left\{\frac{dc_p}{dT}(-WD_3(T) - UD_1(T)) + i\left[\frac{(\gamma-1)}{\gamma} - c_p\right]\xi\right\} + \\
&\quad \frac{(\gamma-1)}{\gamma}(UD_1(\rho) + WD_3(\rho)) + \\
&\quad \frac{(\gamma-1)}{R}\frac{d\mu}{dT}M^2\left[(D_3(U))^2 + (D_3(V))^2\right] + \\
&\quad \frac{1}{R\,\mathrm{Pr}}\left[\frac{d\kappa}{dT}D_{33}(T) + \frac{d^2\kappa}{dT^2}(D_3(T))^2 + \kappa(-\beta_0^2 - \alpha_0^2)\right] \\
b(1,1) &= W \\
b(1,4) &= \rho \\
b(2,2) &= \rho W - \frac{1}{R}\frac{d\mu}{dT}D_3(T)
\end{aligned}
$$

$$
\begin{aligned}
b(2,4) &= -\frac{i\mu}{R}\alpha_0 l_1 \\
b(2,5) &= -\frac{1}{R}D_3(U)\frac{d\mu}{dT} \\
b(3,3) &= \rho W - \frac{1}{R}\frac{d\mu}{dT}D_3(T) \\
b(3,4) &= -\frac{i\mu}{R}\beta_0 l_1 \\
b(3,5) &= -\frac{1}{R}D_3(V)\frac{d\mu}{dT} \\
b(4,1) &= \frac{1}{\gamma M^2}T + \frac{i\mu}{R}\frac{l_2}{\rho}\xi \\
b(4,2) &= \frac{i\mu}{R}\alpha_0 \\
b(4,3) &= \frac{i\mu}{R}\beta_0 \\
b(4,4) &= \rho W + \frac{l_2}{R}(2\mu\frac{D_3(\rho)}{\rho} - \frac{d\mu}{dT}D_3(T)) \\
b(4,5) &= \frac{1}{\gamma M^2}\rho \\
b(5,1) &= \frac{(\gamma-1)}{\gamma}WT \\
b(5,2) &= 2(\gamma-1)M^2\frac{\mu}{R}D_3(U) \\
b(5,3) &= 2(\gamma-1)M^2\frac{\mu}{R}D_3(V) \\
b(5,5) &= \rho W\left[\frac{(\gamma-1)}{\gamma} - c_p\right] + \frac{2}{R\,\mathrm{Pr}}\frac{d\kappa}{dT}D_3(T) \\
c(2,2) &= -\frac{\mu}{R} \\
c(3,3) &= -\frac{\mu}{R} \\
c(5,5) &= \frac{\kappa}{R\,\mathrm{Pr}} \\
d(1,1) &= U \\
d(1,2) &= \rho \\
d(2,1) &= \frac{T}{\gamma M^2} \\
d(2,2) &= \rho U \\
d(2,5) &= \frac{\rho}{\gamma M^2} \\
d(3,3) &= \rho U
\end{aligned}
$$

$$
\begin{aligned}
d(4,4) &= \rho U \\
d(5,1) &= \frac{(\gamma-1)}{\gamma} UT \\
d(5,5) &= \rho U \left[\frac{(\gamma-1)}{\gamma} - c_p \right]
\end{aligned}
$$

where

$$D_i = \frac{1}{h_i}\frac{\partial}{\partial x^i}, \quad D_{ij} = \frac{1}{h_i h_j}\frac{\partial^2}{\partial x^i \partial x^j}, \quad \alpha_0 = \frac{\alpha}{h_1}, \quad \beta_0 = \frac{\beta}{h_2}, \quad l_j = \frac{\lambda}{\mu} + j,$$

and

$$\xi = (\alpha_0 U + \beta_0 V - \omega).$$